Fibers and Polymers 2017, Vol.18, No.3, 502-513
DOI 10.1007/s12221-017-6988-z

ISSN 1229-9197 (print version)
ISSN 1875-0052 (electronic version)

Electrospun Polyindole Nanofibers as a Nano-adsorbent for Heavy Metal Ions Adsorption for Wastewater Treatment

Zhijiang Cai[1,2]*, Xianyou Song[1], Qing Zhang[1], and Tingting Zhai[1]

[1]*School of Textiles, Tianjin Polytechnic University, Tianjin 300387, China*
[2]*Key Laboratory of Advanced Textile Composites, Ministry of Education of China, Tianjin 300387, China*
(Received October 10, 2016; Revised January 9, 2017; Accepted January 12, 2017)

Abstract: Polyindole nanofibers were prepared via electrospinning method using acetonitrile as solvent. The obtained electrospun polyindole nanofibers were characterized with SEM, TEM, FTIR and BET surface areas measurements. Adsorption experiments were carried out in batch sorption mode to investigate the effect of pH, contact time and diameter of polyindole nanofibers. The Cu(II) adsorption was highly pH dependent and the optimum pH was found to be 6. The maximum adsorption capacities for electrospun polyindole nanofibers and polyindole powders were 121.95 and 18.93 mg/g attained in 15 and 60 min, respectively. With the diameter of polyindole nanofibers increasing, the adsorption capacity slightly decreased. The adsorption isotherm data fitted well to the Langmuir isothermal model which indicates that the monolayer adsorption occurred. The kinetics data analysis showed that the adsorption process could be described by pseudo-second order kinetic model, suggesting a chemisorption process as the rate limiting step. Thermodynamic parameters ΔH^o, ΔS^o and ΔG^o for the Cu(II) adsorption by polyindole nanofibers were calculated. The results showed that the Cu(II) adsorption was feasible, spontaneous and endothermic. Desorption results revealed that the adsorption capacity can remain up to 75 % after 10 times usage. The electrospun polyindole nanofibers would have promising application for removal of Cu(II) from wastewater treatment.

Keywords: Polyindole, Electrospinning, Nanofiber, Cu(II), Adsorption

Introduction

Heavy metal ions have become a serious threat to human beings and environments due to their toxicity, non-biodegradability and accumulation characteristics in nature. Cu(II) is one of the widely existed heavy metal ions in wastewater which may come from various industrial sources such as printed circuit boards, electroplating, metal finishing, textile, paper industries and etc [1,2]. Excess intake of Cu(II) may lead to various ailments such as nausea, stomachache, gastrointestinal disturbance, neurological dysfunction, hemolysis, liver and kidney damage [3,4]. Thus, the removal of Cu(II) from wastewater is becoming an important issue. There are various methods which have been developed for the removal of heavy metal ions such as solvent extraction, membrane separation, adsorption, flocculation, reverse osmosis and filtration, ion exchange, etc [5-8]. Among all these methods, adsorption is the most commonly and widely studied method for removal of metal ions from solutions. To adsorb metal ions effectively from aqueous solutions, various materials have been utilized as adsorbents such as activated carbon, oxide minerals, polymer materials, resins, biosorbents, etc [9-12].

Conducting polymers have attracted much interest in the past 20 years because they simultaneously display the physical and chemical properties of organic polymers and the electrical characteristics of metals. The main work of conducting polymers focuses on heterocyclic conducting polymers containing nitrogen atoms like polyaniline, polypyrrole and their substituted derivatives. They have also been investigated for many industrial applications such as electromagnetic shielding, actuators, chemical sensors and polymer batteries [13-16]. In recent year, the use of conducting polymers for water treatment has also been proposed. They have shown good prospect for removing heavy metal ions from aqueous solution due to the presence of nitrogen atoms which can chelate metal ions through electrostatic [17].

Olad *et al.* [18,19] have reported the removal of toxic Cr(VI) in aqueous solution by using polyaniline as adsorbents. The ability of polyaniline coated sawdust as synthetic adsorbent has also been investigated for Cd(II) removing from aqueous solutions [20]. Omraei *et al.* [21] have investigated the removal of Zn(II) from aqueous solutions using polypyrrole coated sawdust as adsorbent.

However, the removal efficiency for metal ions in these studies is rather low. It is desirable to develop an adsorbent with high removal capacity as well as relatively faster adsorption rate for practical application. To approach this object, the nanotechnology has been utilized to fabricate the nano-adsorbents with enhanced adsorption capacity and rapid adsorption rate due to the large surface areas and more active sites.

Electrospinning technique provides a versatile and effective method to prepare fibers with the diameters ranging from the nano to micro-meter scale. The electrospun fibers have exceptionally long length, uniform diameter, high porosity, interconnectivity, interstitial and large specific surface ratio, which can be applied in membrane filtration technology [22], tissue engineering [23] wound dressings [24], optical sensors and biosensors [25], and metal ions adsorption [26].

*Corresponding author: caizhijiang@hotmail.com

Especially, the application of electrospun nanofibers in heavy metal removal has attracted numerous attentions. Chitosan nanofiber membranes prepared by electrospinning have been used for the adsorption of Pb(II), Cd(II) and Cr(VI) [27-29]. Chitosan composite nanofiber membranes such as Chitosan/poly(ethylene oxide) and Chitosan/(polyvinyl alcohol)/zeolite have also been developed for Cr(VI), Fe(III), Pb(II), Cd(II) and Ni(II) adsorption [30-32]. Cellulose-based electrospun nanofiber membranes such cellulose/silk fibroin blend [33], cellulose/polyvinylpyrrolidone blend [34] and surface functionalized cellulose nanofiber membranes such as oxolane-2,5-dione modified electrospun cellulose [35], poly(methacrylic acid) modified electrospun cellulose [36] have been investigated for Cu(II), Cd(II), Pb(II) and Hg(II) adsorption. Also, electrospun polyacrylonitrile nanofibers membranes treated by hydrolysis [37,38], amination [39,40], amidoxime [41-43] have been fabricated and their adsorption performances for Ni(II), Cu(II), Pb(II), U(VI), Ag(II), Fe(II) and Au(III) have been studied. Electrospun polyvinylpyrrolidone (PVP) based composite nanofiber membranes such as PVP/SiO_2 [44], PVP/Si/3-aminopropyl-triethoxysilane [45], and PVP/CeO_2 [46] have been reported for their application for Cr(III), Pb(II) and Cu(II) removal from wastewater. Electrospun poly(vinyl alcohol) (PVA) nanofiber and PVA-based composite nanofibers such as PVA/hydroxyapatite [47], PVA/ZnO [48], PVA/TiO_2/ZnO [49], PVA/zeolite [50] have been prepared and used in Zn(II), Ni(II), U(VI), Cu(II), Th(IV) and Cd(II) adsorption. These studies manly focus on the electrospun non-conducting polymer nanofibers. Recently, electrospun polyaniline nanofibers and polyaniline nanofibers assembled on alginate microsphere have been prepared as nano-adsorbents for the removal of Cu(II), Pb(II) and Cr(VI) from aqueous solution [51,52]. Polypyrrole-coated electrospun nanofiber membranes and polypyrrole/polyacrylonitrile nanofibers have been prepared as nano-adsorbents for Au(III) and Cr(VI) adsorption from aqueous solution [53,54].

Polyindole is a conducting polymer, which can be obtained by electrochemical oxidation or chemical polymerization. Polyindole exhibits the properties of both poly(para-phenylene) and polypyrrole together, such as fairly good thermal stability [55], high-redox activity and stability [56], slow degradation rate in comparison with polyaniline and polypyrrole [57], and air stable electrical conductivity [58]. In this paper, polyindole nanofibers were prepared using the electrospinning technique and applied to adsorb the Cu(II) from aqueous solution. The Cu(II) concentration in the solution was measured by atomic absorption spectroscopy. The adsorption performances for Cu(II) were investigated.

Experimental

Chemicals

The materials used in this investigation and their sources are as follows: polyindole powder was chemically synthesized by our lab using the same procedures as reported previously [59]. Acetonitrile, $CuSO_4$, base (NaOH) and acid (HNO_3) were obtained from Sigma Chemical Co., Ltd. and used as received. All other chemicals employed were of analytical reagent grade. Distillated water was used for all preparation and washing stages.

Electrospinning of Polyindole Nanofibers

Polyindole solution was prepared by dissolving polyindole powder in acetonitrile under ultrasonification and then filtered through Teflon membrane. Electrospinning of polyindole was then carried out as the following procedures. Polyindole solution was filled into a glass syringe terminated by a stainless steel needle whose inner diameter is 0.35 mm. The syringe was placed in an automatic pump and polyindole solution was extruded out at a speed of 0.5 m*l*/h. High voltage ranging from 20 to 28 kV was applied in the electrospinning process. The tip-to-collector distance was fixed at 20 cm. The polyindole nanofibers were collected by Aluminum foil. The experiment was done in an environmental chamber with constant temperature at 25 ^{o}C and the relative humidity (RH) at 50 %. The electrospinning parameters were selected based upon previous research by our lab [60] and the sample codes were listed in Table 1.

Characterization

Viscometer (Brookfield Corporation DV-II) was used to measure the viscosity of polyindole solution prior to electrospinning. The surface morphology of the obtained polyindole nanofibers was observed by scanning electron microscopy (SEM, Model S-4200, Hitachi, Japan) and transmission electron microscopy (TEM, JEM-1200EX, Japan). The Brunauer-Emmett-Teller (BET) method was used to measure the pore volume, pore diameter and specific surface area by a surface area analyzer (SAA: Sorptomatic 1990, ThermoFinnigan Co.). The FTIR spectra were recorded using a Perkin Elmer Spectrum RX-I spectrophotometer with the KBr pellet technique. A model 939 Unicam atomic absorption spectrophotometer (AAS) was used to determine the Cu(II) concentration. The pH levels were measured with a pH-meter from Hach Co. (United States).

Adsorption Equilibrium Experiments

Adsorption equilibrium experiments were carried out in a temperature controlled thermostatic shaker operated at

Table 1. Electrospinning parameters for polyindole

Sample code	Concentration (%)	Viscosity (cP)	Humidity (%)	Temperature (^{o}C)	Voltage (kV)
PIN-1	2.0	800	50	25	20
PIN-2	1.8	775	50	25	24
PIN-3	1.6	750	50	25	28

200 rpm. All the Cu(II) solutions required for experiments were freshly prepared by diluting the stock solution. The effect of pH on Cu(II) adsorption by the polyindole nanofibers was evaluated and compared with polyindole powders. The pH of the Cu(II) solution in the range of 2-8 was adjusted by using 1-0.1 mol/*l* HNO_3 or 1-0.1 mol/*l* NaOH. The initial concentration of Cu(II) solution was 100 mg/*l* and the amount of adsorbent was 0.05 g. Then, samples of polyindole nanofibers were added to 50 m*l* of a Cu(II) solution stirred at 120 rpm at 20 °C for 2, 4, 6, 8, 10, 12, 14, 16, 18, 20, 25, 30, 40, 60, 90 and 120 min. Finally, the polyindole nanofibers adsorbent was separated from solution by filtration and the filtrate was analyzed for residual Cu(II) concentrations by AAS analysis. The equilibrium sorption capacity (q_e) (mg/g) of the polyindole nanofibers adsorbent for Cu(II) was calculated as follows:

$$q_e = \left(\frac{C_0 - C_e}{m}\right) \times V \quad (1)$$

where V is the solution volume (L), m is the amount of added adsorbent (g), C_o and C_e are the initial and equilibrium Cu(II) concentrations (mg/*l*), respectively.

Adsorption Isotherms

Sorption isotherms at three temperatures (20, 30 and 40 °C) were investigated at pH 6 by changing the initial concentration of Cu(II) from 100 to 400 mg/*l*. The procedure was similar to that described for the adsorption equilibrium experiments.

Desorption and Recyclability

For desorption, 0.1 g polyindole nanofibers was first contacted with 200 m*l* 100 mg/*l* Cu(II) solution for 12 h at optimum pH and 40 °C. Then the polyindole nanofibers were rinsed with distilled water to remove residual solution. After that, the desorption experiments were performed by immersing the Cu(II) loaded nanofibers into 100 m*l* 1 mol/*l* HNO_3 aqueous solutions and shaking for 2 h. The desorption efficiency (%) was calculated based on the percentage of the ratio between the desorbed and pre-adsorbed amounts of the metal ions. The recyclability of polyindole nanofibers was evaluated by repeating the above processes for 10 times.

Results and Discussion

Morphology of the Polyindole Nanofibers

The morphology of electrospun polyindole nanofibers was observed by SEM and TEM as shown in Figure 1. Electrospun polyindole nanofibers exhibit smooth surfaces, round shape and random orientation. The polyindole nanofibers have average submicron fiber diameter ranged from 140 nm to 300 nm calculated as an average value from 100 measurements using Image Pro Plus software. A TEM image for PIN-3 is shown in Figure 1(d). It can be seen that the polyindole nanofiber shows a regular round shape structure with diameter about 140 nm. The surface of the nanofiber is smooth and there are no pores on it. The average fiber diameter together with pore volume, pore diameter and specific surface areas of the polyindole nanofibers are summarized in Table 2. With the applied voltage increasing, the average fiber diameter tends to decrease. The pore volume, pore diameter and specific surface areas are in the range of 0.217-0.250 $cm^3\ g^{-1}$, 55-68 nm and 64.43-86.41 $m^2\ g^{-1}$, respectively, depending on the fiber diameter. With the fiber diameter decreasing, the pore volume and the specific surface areas increase while the pore diameter decreases. The thinnest fiber with diameter of 140 nm can be fabricated in this work. By optimization the electrospinning parameters, thinner polyindole fibers with diameter less than 100 nm can be fabricated. This kind of work is ongoing in our lab and the results will be reported later.

Adsorption Behaviors

Effect of pH

The pH level is considered as one of the most important parameters that influence the adsorption behavior of metal ions in aqueous solutions. The effect of solution pH lies in the solubility of the metal ions in the solution, the degree of ionization of the adsorbate and replacement some of the positive ions in the active sites. In this study, the effect of pH on the adsorption of Cu(II) by electrospun polyindole nanofibers was evaluated within the pH range of 2-8 and the results were shown in Figure 2. At low pH level (less than 2), the adsorption capacity is very small due to the lots of protonated amino groups which make the Cu(II) unable to be bonded by active sites of the electrospun polyindole nanofibers. At high pH levels (e.g., 9-12), the precipitation of the Cu(II) as hydroxides in the form of $Cu(OH)_2$ would take place. It has been shown that Cu(II) reaches maximum adsorption capacity at pH 6 and the adsorption capacity decreases by either raising or lowering pH. At lower pH values, the H^+ concentration is high and the hydronium ions will compete with metal ions for the adsorption sites. What's more, the adsorbed hydrogen ions will repel the metal ions. Thus, the pH value is set to 6 for subsequent adsorption experiments.

Effect of Diameter of Nanofibers

Figure 3 shows the results of adsorption capacity for Cu(II) by electrospun polyindole nanofibers with different average diameter ranged from 140 nm to 300 nm. With the diameter increasing, the adsorption capacity of Cu(II) decreases and the equilibration time of Cu(II) adsorption increases. The adsorption capacity for Cu(II) adsorption by PIN-1, PIN-2 and PIN-3 is 77.36, 85.11 and 93.37 mg/g attained in 20, 17 and 15 min, respectively. Consequently, the smaller diameter of the nanofibers results in higher adsorption capacity and adsorption rate. Thus, the PIN-3 with average diameter of 140 nm is used for subsequent

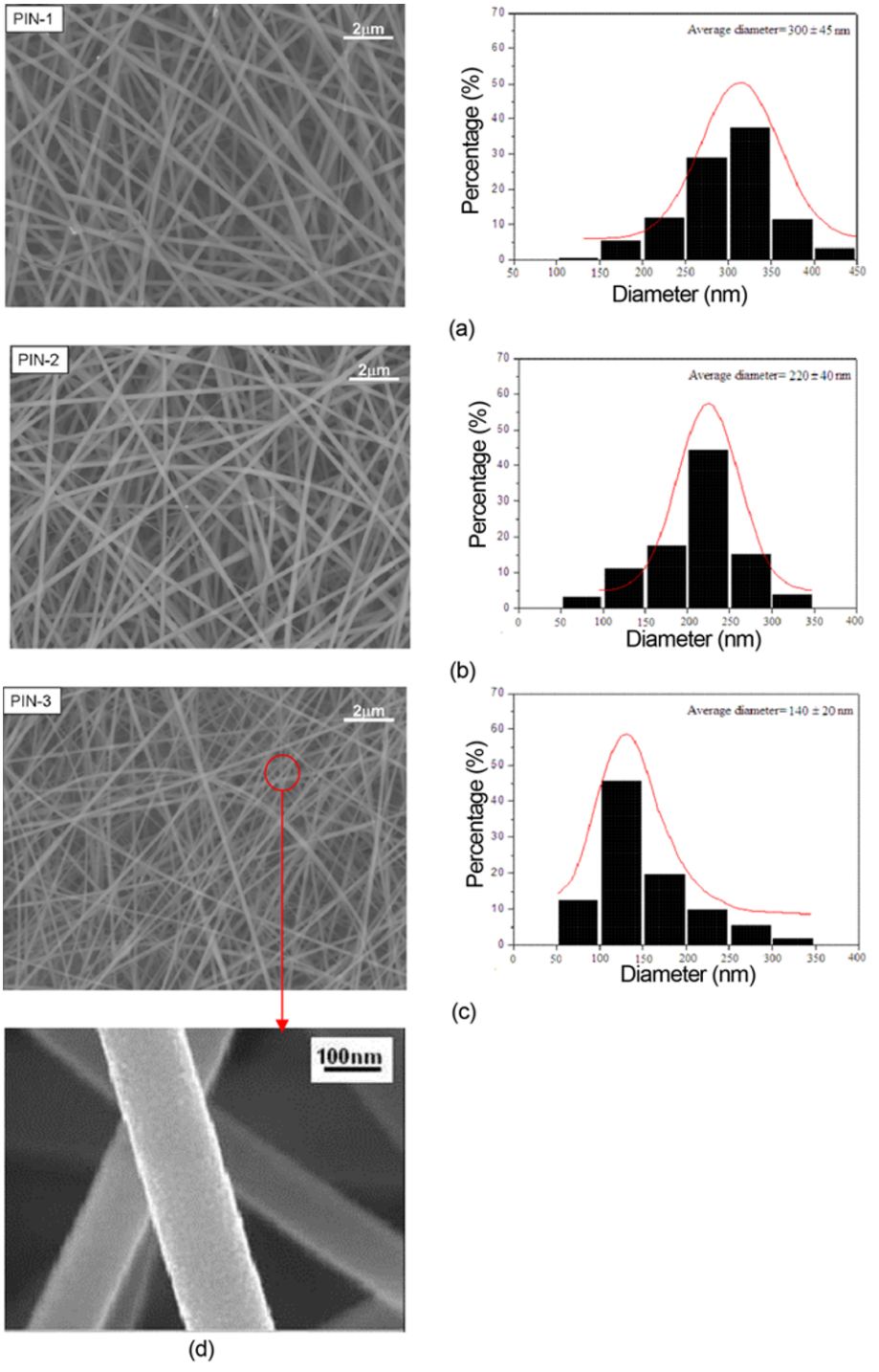

Figure 1. SEM and TEM images and fiber diameter distribution of the electrospun polyindole nanofibers; (a) PIN-1, (b) PIN-2, (c) PIN-3, and (d) TEM (PIN-3).

adsorption experiments.

Effect of Contact Time

In order to evaluate the equilibration time for adsorption capacity and the kinetics of the adsorption process, Cu(II) adsorption by electrospun polyindole nanofibers and polyindole powders was investigated as a function of contact time (for 2 h) and the results were shown in Figure 4. The amount of Cu(II) adsorption by electrospun polyindole nanofibers increases rapidly in the first 15 min and then levels off. However, the equilibration time for polyindole powders is

Table 2. Physical properties of the electrospun polyindole nanofibers

Samples code	Average fiber diameter (nm)	Pore volume ($cm^3\ g^{-1}$)	Pore diameter (nm)	Specific surface area ($m^2\ g^{-1}$)
PIN-1	300	0.217	68	64.43
PIN-2	225	0.231	64	71.67
PIN-3	140	0.250	55	86.41

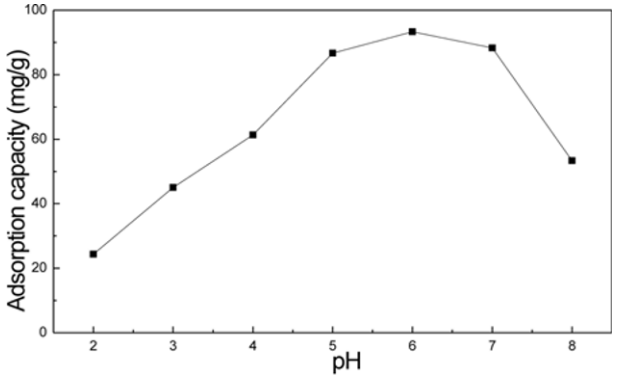

Figure 2. Effect of solution pH on the Cu(II) adsorption by the polyindole nanofibers (Cu(II) concentration: 100 mg/*l*, volume: 50 m*l*, contact time: 1 h, the diameter of the polyindole nanofibers: 140 nm, temperature: 20 °C).

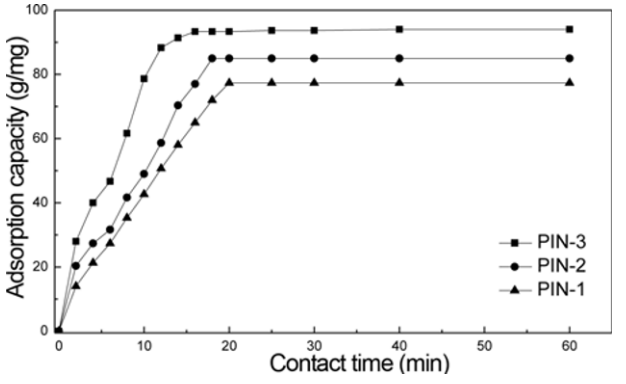

Figure 3. Effect of diameter of the polyindole nanofibers on the Cu(II) adsorption (Cu(II) concentration: 100 mg/*l*, volume: 50 m*l*, pH: 6, contact time: 60 min, temperature: 20 °C).

four times longer. The maximum adsorption capacity for polyindole nanofibers and powders is 93.37 and 18.93 mg/g attained in 15 and 60 min, respectively. The polyindole nanofibers exhibit a five times larger adsorption capacity and a four times faster adsorption rate compared with that of the polyindole powders. The reason might be attributed to its higher specific surface areas which can provide more adsorption sites. For the following experiments, the contact time is fixed to 60 min to ensure the equilibrium adsorption.

Effect of other Metal Ions

In general, Na^+, K^+, Mg^{2+} and Ca^{2+} can be detected in

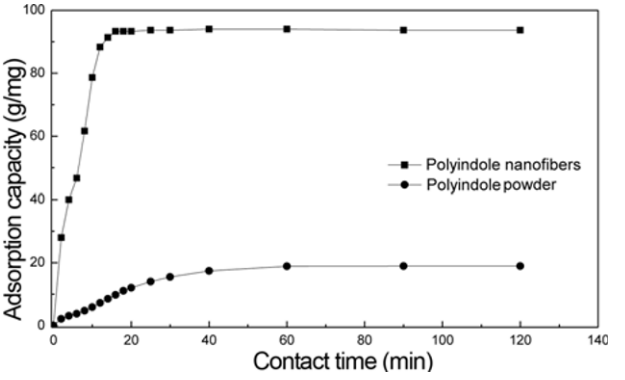

Figure 4. Effect of contact time on the Cu(II) adsorption by the polyindole nanofibers and polyindole powders (Cu(II) concentration: 100 mg/*l*, volume used 50 m*l*, pH: 6, the diameter of the polyindole nanofibers: 140 nm, temperature 20 °C).

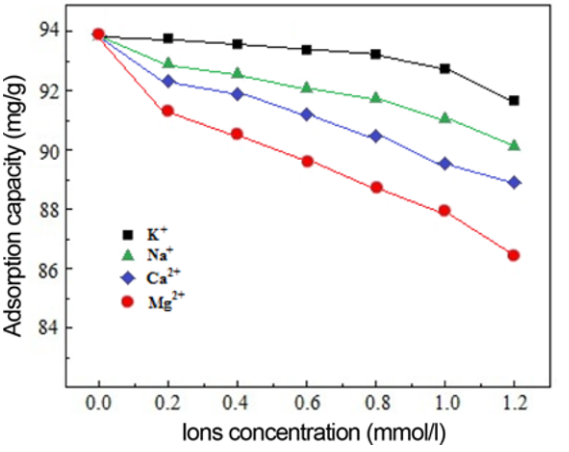

Figure 5. Effect of other metal ions on the Cu(II) adsorption by the polyindole nanofibers (Cu(II) concentration: 100 mg/*l*, volume: 50 m*l*, pH: 6, the diameter of the polyindole nanofibers: 140 nm, temperature: 20 °C).

various industrial wastewaters. The exist of Na^+, K^+, Mg^{2+} and Ca^{2+} results in high ionic strength, which may affect the adsorption behavior. Adsorption experiments were performed using NaCl, KCl, $MgCl_2$ and $CaCl_2$ aqueous solution with ions concentration in the range of 0-1.2 mmol/*l* to investigate the effect of ionic strength on Cu(II) adsorption capacity. The experiments were carried out at initial Cu(II) concentration 100 mg/*l*, solution pH 6 and 20 °C for 60 min. Figure 5 demonstrates that with ions concentration increasing from 0 to 1.2 mmol/*l*, the Cu(II) adsorption capacity by polyindole nanofibers decreases from 93.37 mg/g to 91.72 mg/g for KCl, 90.24 mg/g for $CaCl_2$, 88.91 mg/g for NaCl and 86.52 mg/g for $MgCl_2$, respectively. The reason might be due to the fact that Na^+, K^+, Mg^{2+} and Ca^{2+} belong to cations which can compete with Cu(II) for the same adsorption active sites on the surface of the polyindole nanofibers. However, the adsorption capacity is slightly affected under

the low ions concentrations.

Adsorption Isotherms

Adsorption isotherms were studied at three different temperatures to investigate the Cu(II) adsorption capacity by the electrospun polyindole nanofibers. Langmuir, Freundlich and Temkin models, the most commonly used solid-liquid phase isotherms, were used to describe the relationship between the Cu(II) in solution and the electrospun polyindole nanofibers.

The Langmuir (equation (2)), Freundlich (equation (3)) and Temkin (equation (4)) model have the general form:

$$\frac{C_e}{q_e} = \frac{1}{q_m K_L} + \frac{C_e}{q_m} \tag{2}$$

$$\ln q_e = \ln K_f + \frac{\ln C_e}{n} \tag{3}$$

$$q_e = \frac{RT}{B_T}\ln K_T + \frac{RT}{B_T}\ln C_e \tag{4}$$

where C_e (mg/*l*) is the equilibrium concentration of the metal ion, q_e (mg/g) is the adsorption capacity in equilibrium state, q_m (mg/g) is the maximum adsorption capacity, K_L (*l*/mg) is the Langmuir constant related to the energy of adsorption, K_f and n are the Freundlich isotherm parameters related to adsorption capacity (mg/g) and intensity of adsorption, respectively. K_T (*l*/g) is the equilibrium binding constant corresponding to the maximum binding energy, B_T (kJ/mol) is the Temkin constants related to the heat of adsorption, R (8.314 J/mol/K) is the universal gas constant and T (K) is the absolute temperature.

Figure 6 presents the adsorption isotherms of Cu(II) by the electrospun polyindole nanofibers as a function of equilibrium concentration at solution temperature of 20, 30 and 40 °C. As seen from the Figure 6, the adsorption capacity increases with solution temperature increasing. The reason could be attributed to an increase in thermal energy of the adsorbing species, which can increase the chemical interactions between the adsorbate ions and active sites of the adsorbent. In return, it results in higher adsorption capacity and faster adsorption rate. This result confirms that the Cu(II) adsorption by the polyindole nanofibers is endothermic.

Figure 7 displays the linearized Langmuir, Freundlich and

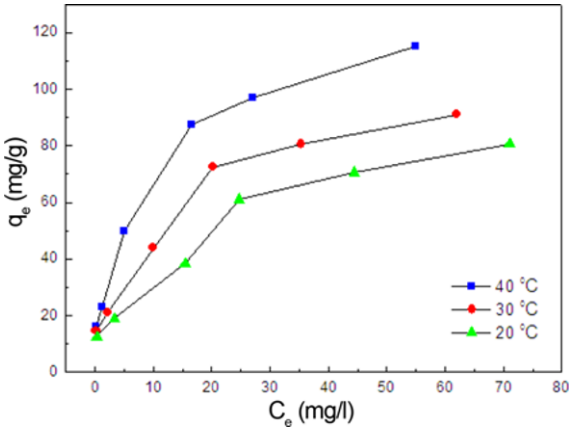

Figure 6. Equilibrium isotherms of the Cu(II) adsorption by the polyindole nanofibers at different temperature (pH: 6, contact time: 60 min, the diameter of the polyindole nanofibers: 140 nm).

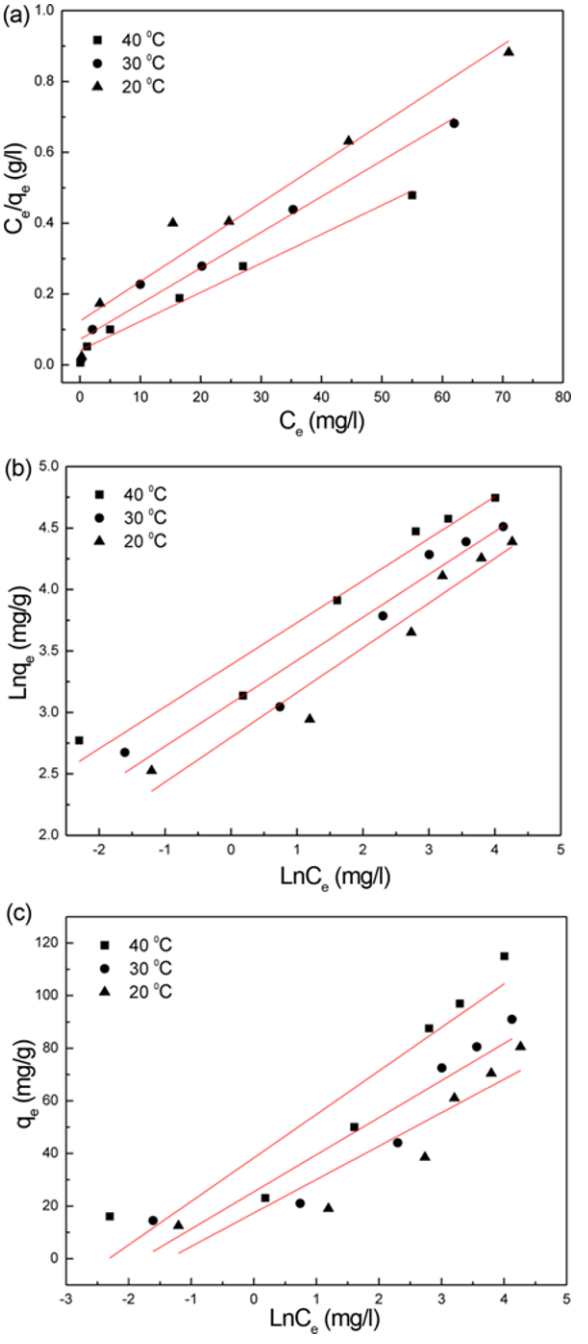

Figure 7. Fit of equilibrium data to Langmuir isotherm model (a), Freundlich isotherm model (b) and Temkin isotherm model (c) for the Cu(II) adsorption by the electrospun polyindole nanofibers.

Table 3. Langmuir, Freundlich and Temkin isotherm parameters for Cu(II) adsorption by the electrospun polyindole nanofibers

Temperature	Langmuir model			Freundlich model			Temkin model		
(°C)	q_m (mg/g)	K_L (*l*/mg)	R^2	K_f (mg/g)	n	R^2	K_T (*l*/g)	B_T (kJ/mol)	R^2
20	88.50	0.090	0.940	16.41	2.75	0.931	3.92	191.66	0.812
30	99.11	0.141	0.970	21.63	2.86	0.936	6.06	178.65	0.842
40	121.95	0.201	0.982	29.63	2.93	0.944	10.15	157.40	0.860

Temkin isotherms. The isotherm parameters at three different temperatures are analyzed from the plots and summarized in Table 3. The correlation coefficient (R^2) is used to evaluate the fitness of the three models. The results reveal that the data agree strongly with Langmuir adsorption isotherm model (R^2=0.940 at 20 °C, 0.970 at 30 °C and 0.982 at 40 °C) compared to the Freundlich (R^2=0.931 at 20 °C, 0.936 at 30 °C and 0.944 at 40 °C) and Temkin models (R^2=0.812 at 20 °C, 0.842 at 30 °C and 0.860 at 40 °C). The value of *qm* for the Cu(II) adsorption by the polyindole nanofibers calculated from the Langmuir model increases from 88.50 to 121.95 mg/g with the temperature increasing from 20 to 40 °C, consistent with the actual saturated adsorption capacity (80.50 mg/g at 20 °C, 91.64 mg/g at 30 °C and 117.84 mg/g at 40 °C). The value of *KL* increases from 0.09 to 0.201 with the temperature increasing from 20 to 40 °C, suggesting the stronger affinity of the polyindole nanofibers for Cu(II) adsorption at higher temperature.

Adsorption Thermodynamics

To study the thermodynamics of Cu(II) adsorption by electrospun polyindole nanofibers, the thermodynamic parameters such as standard Gibbs free energy change (ΔG^o), enthalpy change (ΔH^o) and entropy change (ΔS^o) were evaluated by the Van't Hoff equation (equation (5)), which correlates ΔH^o and ΔS^o with Langmuir equilibrium constant, *KL*.

$$\ln K_L = \frac{\Delta S^o}{R} + \frac{-\Delta H^o}{RT} \quad (5)$$

The slope, $\Delta H^o/R$ and the intercept $\Delta S^o/R$ obtained by plotting $\ln K_L$ *vs 1/T* (Figure 8) according to equation (5) give ΔH^o and ΔS^o values, which are listed in Table 4. On the basis of the values of K_L as a function of temperatures, ΔG^o values are calculated by equation (6) and reported in Table 4.

$$\Delta G^o = -RT\ln K_L \quad (6)$$

The positive value of ΔH^o and ΔS^o indicates that the adsorption process is endothermic and randomness is increased at the polyindole nanofibers - solution interface during the fixation of the Cu(II) on the active sites of the polyindole nanofibers. All ΔG^o are negative which clearly confirm the feasibility of the process and the spontaneity of the adsorption events. With the temperature increasing, the degree of spontaneity increases, which is primarily due to chemisorption rather than physisorption [61].

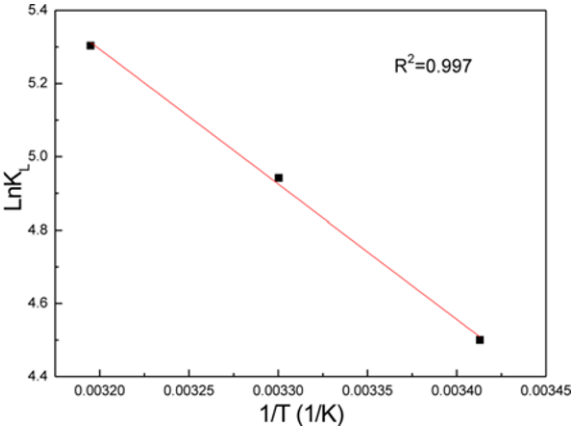

Figure 8. Plot to determine thermodynamic parameters of the Cu(II) adsorption by the polyindole nanofibers.

Table 4. Thermodynamic parameters for Cu(II) adsorption by the electrospun polyindole nanofibers

	ΔH^o (kJ/mol)	ΔS^o (kJ/mol)	R^2	Temperature (°C)	ΔG^o (kJ/mol)
Cu(II)	30.65	0.142	0.944	20	-10.96
				30	-12.47
				40	-13.80

Adsorption Kinetics

The Lagergren's pseudo-first-order and pseudo-second-order model are used to investigate the adsorption kinetic of Cu(II) sorption by the electrospun polyindole nanofibers. The pseudo-first-order model assumes diffusion is the rate limiting step of the adsorption process. The pseudo-second-order model assumes chemisorption as the rate limiting step. The pseudo-first-order (equation (7)) and the pseudo-second-order (equation (8)) can be linearly expressed as follows:

$$\log(q_e - q_t) = \log q_e - \left(\frac{K_1}{2.303}\right)t \quad (7)$$

$$\frac{t}{q_t} = \frac{1}{K_2 q_e^2} + \left(\frac{1}{q_e}\right)t \quad (8)$$

where q_t (mg/g) is the adsorption capacity at time *t* (min), K_1 (1/min) is the pseudo-first-order rate constant, and K_2 (g/mg/

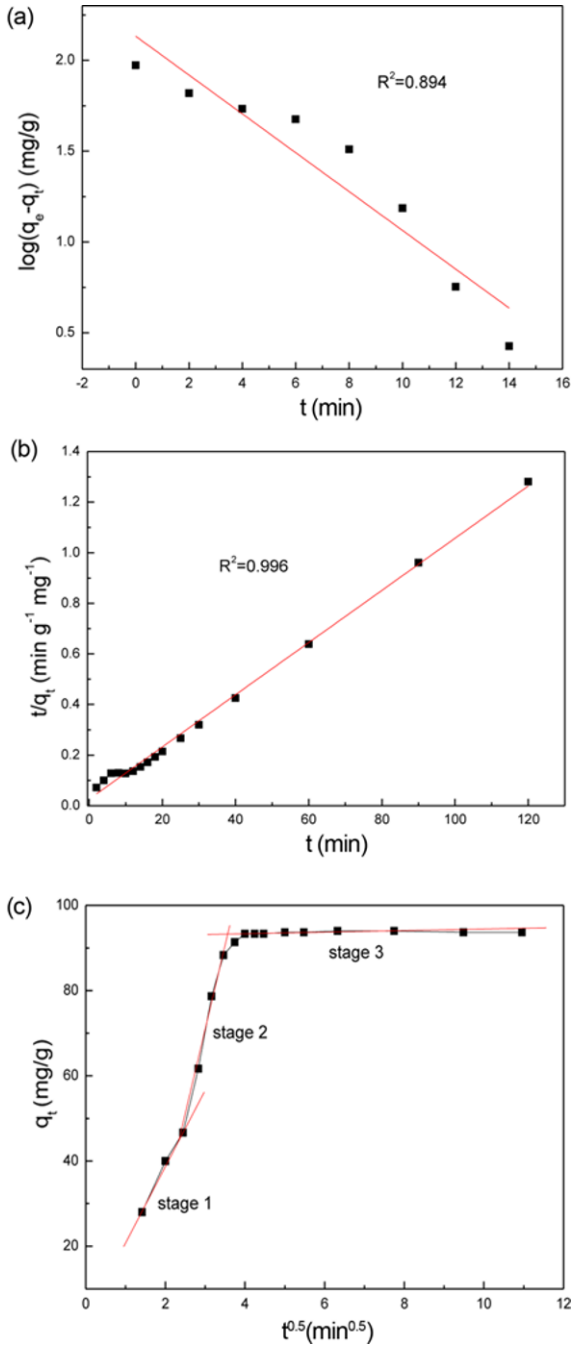

Figure 9. Data fitting for the Cu(II) adsorption by the electrospun polyindole nanofibers using pseudo-first-order kinetic model (a), pseudo-second-order kinetic model (b) and intraparticle diffusion mode (c).

min) is the pseudo-second-order rate constant. The kinetic parameters for pseudo-first-order and pseudo-second-order model are calculated from the intercept and slope of the linear fitting lines by plotting $\log(q_e-q_t)$ *vs* t (Figure 9(a)) and (t/q_t) *vs* t (Figure 9(b)), respectively.

As seen from the results listed in Table 5, the pseudo-second-order model provides better correlation coefficients (R^2=0.995) than the pseudo-first-order model (R^2=0.894). Simultaneously, the good agreement between the calculated $q_{e,cal}$ values (83.45 mg/g) and the experimental $q_{e,exp}$ values (80.50 mg/g) suggests that the adsorption kinetic closely follows the pseudo-second-order model rather than the pseudo-first-order model. This indicates that the rate-limiting step may be chemisorption promoted by covalent/valence forces through exchange or sharing of electrons between adsorbent and adsorbate.

To further analyze the rate-limiting step in adsorption process, intraparticle diffusion model has also been applied. The intraparticle diffusion model can be expressed by the Weber-Morris equation as following:

$$q_t = K_{ip}t^{0.5} + C \tag{9}$$

where K_{ip} (mg/g/min$^{0.5}$) is the intraparticle diffusion rate constant and the intercept C (mg/g) is constant related to the thickness of boundary layer. The values of K_{ip} and C are obtained from the slope and intercept of the linear part of the plot of q_t *vs* $t^{0.5}$ (Figure 9(c)) and listed in Table 5.

The intraparticle diffusion plot (Figure 9(c)) shows multi-linearity and does not pass through the origin suggesting that intraparticle diffusion is not the only rate limiting step. Actually, the intraparticle diffusion plot can be divided into three stages. The steep stage I could be attributed to the rapid transportation of Cu(II) from the solution to the surface of electrospun polyindole nanofibers. The stage II depicts the gradual adsorption process, where intraparticle diffusion is rate-limiting step. The stage III describes the final equilibrium adsorption where intraparticle diffusion begins to decline due to low concentration of Cu(II) in the solution and fewer number of active sites [62]. The three stages in the intraparticle diffusion plot indicate that the Cu(II) adsorption processes by the electrospun polyindole nanofibers involve more than one single kinetic stage.

Desorption and Recyclability

The applicability of extracting Cu(II) from the pre-absorbed polyindole nanofibers was evaluated. Figure 10(A) shows

Table 5. Kinetic parameters for Cu(II) adsorption by the electrospun polyindole nanofibers

Ions	$q_{e,exp}$ (mg/g)	Pseudo-first-order model			Pseudo-second-order model			Intraparticle diffusion model		
		K_1 (1/min)	$q_{e,cal}$ (mg/g)	R^2	K_2 (g/mg/min)	$q_{e,cal}$ (mg/g)	R^2	K_{ip} (mg/g/min$^{0.5}$)	C (mg/g)	R^2
Cu(II)	80.50	0.246	135.83	0.894	0.00406	83.45	0.996	29.94	2.14	0.946

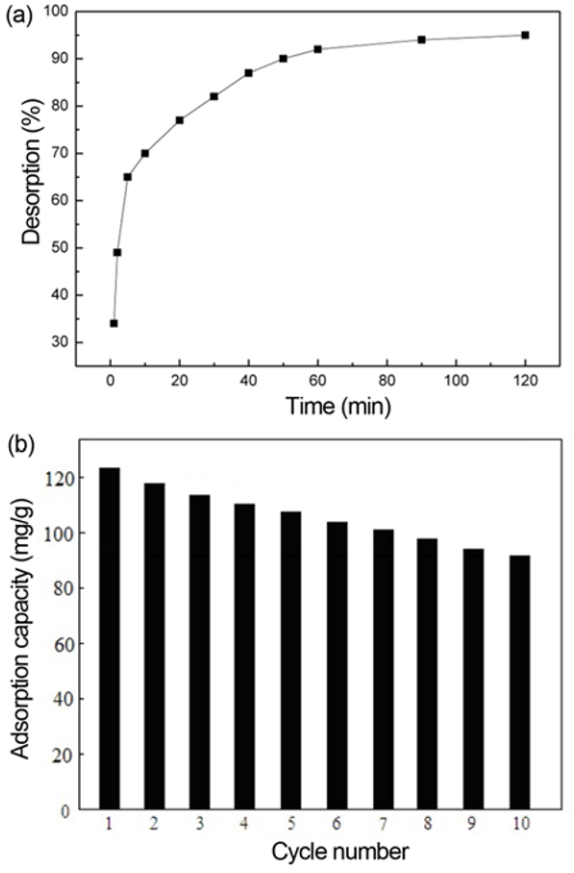

Figure 10. Desorption of Cu(II) from the metal-loaded polyindole nanofibers in a 1 mol/*l* HNO_3 solution as a function of time (a) and adsorption capacity of the electrospun polyindole nanofibers after regeneration (b).

the desorption of Cu(II) in a 1 mol/*l* HNO_3 solution. Cu(II) is desorbed by 70 % within 5 min. The amount of recovered Cu(II) is nearly 90 % after 60 min. This property is vital for the practical application of the polyindole nanofibers as adsorbent. After desorption treatment, the nanofiber is reused to absorb the 100 mg/*l* of Cu(II) in the aqueous solution with pH value of 6, as shown in Figure 10(B). The adsorption capacity at 3th, 5th and 7th cycle is about 116.73, 108.22 and 100.76 mg/g which are about 95 %, 88.7 % and 82 % of the initial capacity of polyindole nanofibers. After ten reuses cycles, the adsorption capacity remains 91.62 mg/g which is about 75 % of the initial capacity. The SEM images of the nanofibers after 3th, 5th, 7th and 10th adsorption-desorption cycles are shown in Figure 11. Some erosions can be observed due to high corrosivity of HNO_3 for the 3th and 5th cycles. Although some nanofibers are broken, the nanofibers adsorbent can keep integrity after 10 cycles. These results strongly suggest that the polyindole nanofibers have a promising potential as a adsorbent for recycling Cu(II) from wastewater.

Adsorption Mechanism

According to the kinetic and isotherm analysis results, it can be concluded that the Cu(II) absorption mechanism by the polyindole nanofibers is chemisorption, which might involve formation of chelation through coordination between the Cu(II) (electron-accepting nature) and the polyindole nanofibers (N-containing groups on the surface, electron-donating nature). Figure 12 presents the possible adsorption mechanism of Cu(II) chelation onto the polyindole chains by the nitrogen atoms.

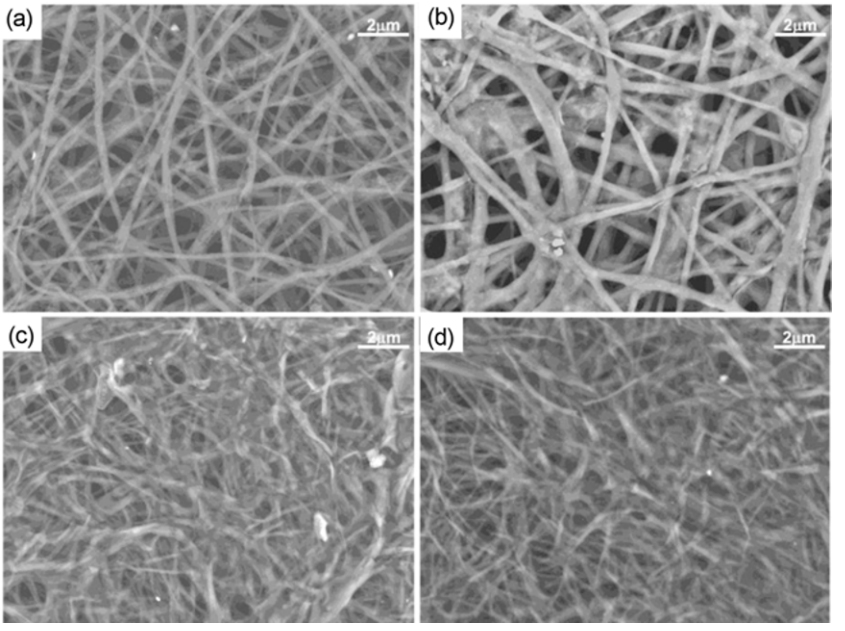

Figure 11. The SEM images of the polyindole nanofibers after 3th (a), 5th (b), 7th (c) and 10th (d) adsorption-desorption cycles.

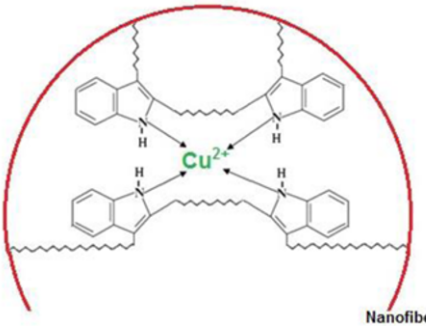

Figure 12. The possible Cu(II) adsorption mechanism by the polyindole nanofibers.

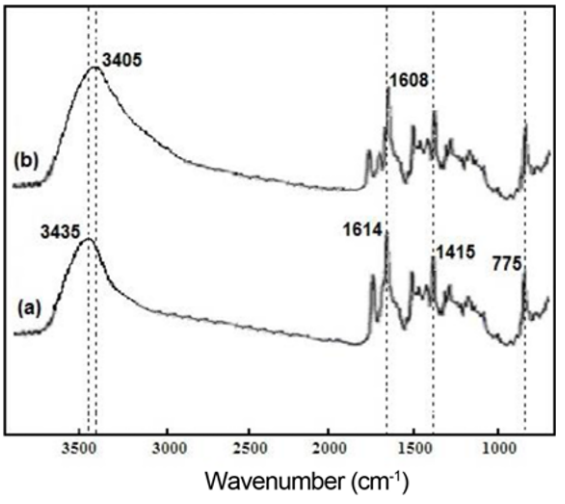

Figure 13. The FTIR spectra of the polyindole nanofibers before (a) and after (b) Cu(II) adsorption.

The FTIR spectra for the polyindole nanofibers before and after Cu(II) adsorption are presented in Figure 13. Before adsorption, a strong and broad band located around 3435 cm^{-1} is ascribed to the characteristic N-H stretching vibrations; the band at 1614 cm^{-1} is assigned to the N-H deformation; the sharp peak at 775 cm^{-1} and 1415 cm^{-1} are attributed to the characteristic out of plane deformations of the C-H bond in the benzene ring and stretching of benzene ring, respectively. After Cu(II) adsorption, the adsorption peaks of N-H at 3435 cm^{-1} and 1614 cm^{-1} shift to 3405 cm^{-1} and 1608 cm^{-1}, respectively. These results indicate that the electro-negativity turns lower for N-H groups which attract electropositive ions such as Cu(II). The FTIR tests confirm that the adsorption mechanism is the chelating of N-H groups with Cu(II).

Comparison of Cu(II) Nanofiber Absorbent

A comparison of the Cu(II) adsorption performance of the different nanofiber absorbents reported by other literatures is summarized in Table 6. The diameter of nanofibers has strong effect on the adsorption performance of adsorbents. It can be seen that the adsorption capacity of the electrospun polyindole nanofibers is comparatively higher than other nanofibers adsorbents. The high adsorption capacity, easy and low cost of the polyindole nanofibers further suggests its potential application in industrial wastewater treatment.

Conclusion

Polyindole nanofibers were prepared via electrospinning method using acetonitrile as solvent and used as nano-adsorbent to removal of Cu(II) from aqueous solution. Adsorption experiments were carried out in batch sorption mode to investigate the effect of pH, contact time and the

Table 6. Comparison of the Cu(II) adsorption capacity of various nanofiber adsorbents

Adsorbent	Diameter of the nanofibers	Operating conditions	Adsorption capacity	Reference
Polyaniline nanofibers assembled on calcium alginate microsphere	30 nm	C_0: 40 mg/*l* pH: 7	67.95 mg/g	[26]
Electrospun polyacrylonitrile nanofibers modified with amidoxime	100-300 nm	C_0: 400 mg/*l* pH: 5.5	52.70 mg/g	[27]
Electrospun silk fibroin/cellulose acetate blend nanofibers	100-600 nm	C_0: 100 mg/*l* pH: -	22.8 mg/g	[33]
Electrospun cellulose/polyvinylpyrrolidone blend nanofibers	500-1200 nm	C_0: 50 mg/*l* pH: 6.0	30.96 mg/g	[34]
Electrospun cellulose acetate nanofibers	500-1500 nm	C_0: 20 mg/*l* pH: 5.7	6.84 mg/g	[36]
Hydrolyzed electrospun polyacrylonitrile fiber mats	135-360 nm	C_0: 200 mg/*l* pH: 5.0	31.3 mg/g	[37]
Aminated electrospun polyacrylonitrile nanofibers	110-205 nm	C_0: 590 mg/*l* pH: 5.0	116.52 mg/g	[39]
Electrospun polyindole nanofibers	140-300 nm	C_0: 100 mg/*l* pH: 6.0	121.95 mg/g	This study

diameter of polyindole nanofibers. The Cu(II) adsorption is highly pH dependent and the optimum pH is found to be 6. The maximum adsorption capacity for polyindole nanofibers and polyindole powders is 121.95 and 18.93 mg/g attained in 15 and 60 min, respectively. With the diameter of polyindole nanofibers increasing, the adsorption capacity slightly decreases. The adsorption isotherm data fit well to the Langmuir isothermal model which indicates that the monolayer adsorption occurred on the surface of nanofibers. Thermodynamic parameters ΔH^o, ΔS^o and ΔG^o for the Cu(II) adsorption by polyindole nanofibers have also been calculated. The results show that the Cu(II) adsorption by the polyindole nanofibers is feasible, spontaneous and endothermic. Desorption results reveal that the adsorption capacity can remain up to 75 % after 10 times usage. It can be concluded that the polyindole nanofibers have potential application for removal of Cu(II) from wastewater.

Acknowledgements

This work is supported by the Tianjin Municipal Science and Technology Foundation (14TXGCCX00014).

Nomenclature

B_T: Temkin constants (kJ/mol)
C: Intraparticle diffusion intercept constant (mg/g)
C_o: Initial Cu(II) concentrations (mg/*l*)
C_e: Equilibrium Cu(II) concentrations (mg/*l*)
K_1: Pseudo-first-order rate constant (1/min)
K_2: Pseudo-second-order rate constant (g/mg/min)
K_L: Langmuir constant parameters (*l*/mg)
K_T: Equilibrium binding constant (*l*/g)
K_f: Freundlich isotherm parameters (mg/g)
K_{ip}: Intraparticle diffusion rate constant (mg/g/min$^{0.5}$)
m: Amount of added adsorbent (g)
n: Intensity of adsorption
q_t: Adsorption capacity at time t (mg/g)
q_e: Equilibrium adsorption capacity (mg/g)
q_m: Maximum adsorption capacity (mg/g)
$q_{e,cal}$: Equilibrium adsorption capacity calculated by kinetic model (mg/g)
$q_{e,exp}$: Equilibrium adsorption capacity obtained by experiment (mg/g)
T: Absolute temperature (K)
t: Time (min)
V: Solution volume (L)
R: The universal gas constant (8.314 J/(K mole))
R^2: Correlation coefficient
ΔG^o: Gibbs free energy change (kJ/mole)
ΔH^o: Enthalpy change (kJ/mole)
ΔS^o: Entropy change (kJ/mole)

References

1. E. Y. Yazici and H. Deveci, *Int. J. Miner Process.,* **134**, 89 (2015).
2. D. P. Chattopadhyay and M. S. Inamdar, *Text. Res. J.*, **84**, 1539 (2014).
3. I. Ali, N. Sakhnini, and I. Naseem, *Biochemistry*, **70**, 1011 (2005).
4. D. Zhang, J. Gao, and K. Zhang, *Biol. Trace Elem. Res.*, **149**, 57 (2012).
5. F. M. Almutairi, P. M. Williams, and R. W. Lovitt, *Desalin. Water Treat*., **42**, 131 (2012).
6. B. Peng, J. Wan, X. Li, Z. Zhang, X. Du, and Z. Lei, *Sep. Sci. Technol*., **47**, 1255 (2012).
7. B. A. Fil, R. Boncukcuoğlu, A. E. Yılmaz, and S. Bayar, *J. Chem. Soc. Pakistan*, **34**, 841 (2012).
8. J. B. Heredia and J. S. Martín, *J. Hazard Mater*., **165**, 1215 (2009).
9. M. Machida, B. Fotoohi, and Y. Amamo, and L. Mercier, *Appl. Surf. Sci.*, **258**, 7389 (2012).
10. G. G. Marisol, R. M. Kardia, and S. Song, *Miner Process Extr. M*, **33**, 301 (2012).
11. B. Li, F. Su, H.K. Luo, L. Liang, and B. Tan, *Micropor. Mesopor. Mat.*, **13**, 207 (2011).
12. U. Farooq, J. A. Kozinski, M. A. Khan, and M. Athar, *Bioresource Technol*., **101**, 5043 (2010).
13. J. D. Sudha, S. Sivakala, R. Prasanth, V. L. Reena, and P. R. Nair, *Compos. Sci. Technol.*, **69**, 358 (2009).
14. G. Alici, V. Devaud, P. Renaud, and G. Spinks, *J. Micromech. Microeng*, **19**, 025017 (2009).
15. L. Xia, Z. Wei, and M. Wan, *J. Colloid Interface Sci.*, **341**, 1 (2010).
16. G. A. Snook, P. Kao, and A. S. Best, *J. Power Sources*, **196**, 1 (2011).
17. R. Ansari, *Acta Chim. Slov.*, **53**, 88 (2006).
18. A. Olada and R. Nabavi, *J. Hazard Mater.*, **147**, 845 (2007).
19. P. A. Kumar, S. Chakraborty, and M. Ray, *Chem. Eng. J*., **141**, 130 (2008).
20. M. S. Mansour, M. E. Ossman, and H. A. Farag, *Desalination*, **272**, 301 (2011).
21. M. Omraei, H. Esfandian, R. Katal, and M. Ghorbani, *Desalination*, **271**, 248 (2011).
22. R. Gopal, S. Kaur, Z. Ma, C. Chan, S. Ramakrishna, and T. Matsuura, *J. Membr. Sci.*, **281**, 581 (2006).
23. Q. P. Pham, U. Sharma, and A. G. Mikos, *Tissue Eng.*, **12**, 1197 (2006).
24. P. Rujitanaroj, N. Pimpha, and P. Supaphol, *Polymer*, **49**, 4723 (2008).
25. K. M. Manesh, P. Santhosh, A. Gopalan, and K. P. Lee, *Anal. Biochem.*, **360**, 189 (2007).
26. S. Haider and S. Y. Park, *J. Membr. Sci.*, **328**, 90 (2009).
27. Y. Li, T. Qiu, and X. Xu, *Eur. Polym. J.*, **49**, 1487 (2013).

28. Y. Li, C. Xu, T. Qiu, and X. Xu, *J. Nanosci. Nanotechnol.*, **15**, 4245 (2015).
29. L. Li, Y. Li, and C. Yang, *Carbohydr. Polym.*, **140**, 299 (2015).
30. U. Habiba, A. M. Afifi, A. Salleh, and B. C. Ang, *J. Hazard Mater.*, **322**, 182 (2017).
31. K. Desai, K. Kit, J. Li, P. M. Davidson, S. Zivanovic, and H. Meyer, *Polymer*, **50**, 3661 (2009).
32. M. Aliabadi, M. Irani, J. Ismaeili, H. Piri, and M. J. Parnian, *Chem. Eng. J.*, **220**, 237 (2013).
33. W. Zhou, J. He, S. Cui, and W. Gao, *Fiber. Polym.*, **12**, 431 (2011).
34. T. Xiang, Z. L. Zhang, H. Q. Liu, Z. Z. Yin, L. Li, and X. M. Liu, *Sci. China Chem.*, **56**, 567 (2013).
35. M. Stephen, N. Catherine, M. Brend, K. Andrew, P. Leslie, and G. Corrine, *J. Hazard Mater.*, **192**, 922 (2011).
36. Y. Tian, M. Wu, R. Liu, Y. Li, D. Wang, J. Tan, R. Wu, and Y. Huang, *Carbohydr. Polym.*, **83**, 734 (2011).
37. P. Kampalanonwat and P. Supaphol, *Ind. Eng. Chem. Res.*, **50**, 11912 (2011).
38. K. Saeed, S. Park, and T. Oh, *J. Appl. Polym. Sci.*, **121**, 869 (2011).
39. P. K. Neghlani, M. Rafizaheh, and F. A. Taromi, *J. Hazard Mater.*, **186**, 182 (2011).
40. P. Kampalanonwat and P. Supaphol, *ACS Appl. Mater. Inter.*, **2**, 3619 (2010).
41. B. Wang, F. Zhang, J. N. Wang, X. Y. Li, and C. J. Li, *Acta Polym. Sin.,* **8**, 1105 (2016).
42. K. Saeed, S. Haider, T. J. Oh, and S. Y. Park, *J. Membr. Sci.*, **322**, 400 (2008).
43. N. Horzum, T. Shahwan, O. Parlak, and M. M. Demir, *Chem. Eng. J.*, **213**, 41 (2012).
44. A. A. Taha, *J. Environ. Sci.*, **24**, 610 (2012).
45. A. R. Keshtkar, A. Tabatabaeefar, A. S. Vaneghi, and M. A. Moosavian, *J. Environ. Chem. Eng.*, **4**, 1248 (2016).
46. S. Yari, S. Abbasizadeh, S. E. Mousavi, M. S. Moghaddam, and A. Z. Moghaddam, *Process Saf. Environ.*, **94**, 159 (2015).
47. A. M. A. El-Aziz, A. El-Maghraby, N. A. Taha, and Arabian, *J. Chem.*. http://dx.doi.org/10.1016/j.arabjc.2016.09.025
48. H. Hallaji, A. R. Keshtkar, and M. A. Moosavian, *J. Taiwan Inst. Chem. E*, **46**, 109 (2015).
49. D. Alipour, A. R. Keshtkar, and M. A. Moosavian, *Appl. Surf. Sci.*, **366**, 19 (2016).
50. L. R. Rad, A. Momeni, B. F. Ghazani, M. Irani, M. Mahmoudi, and B. Noghreh, *Chem. Eng. J.*, **256**, 119 (2014).
51. X. Guo, G. T. Fei, H. Su, and L. D. Zhang, *J. Phys. Chem. C*, **115**, 1608 (2011).
52. N. Jiang, Y. Xu, Y. Dai, W. Luo, and L. Dai, *J. Hazard Mater.*, **215-216**, 17 (2012).
53. J. Wang, K. Pan, Q. He, and B. Cao, *J. Hazard Mater.*, **244-245**, 121 (2013).
54. H. Wang, J. Ding, B. Lee, X. Wang, and T. Lin, *J. Membr. Sci.*, **303**, 119 (2007).
55. D. Billaud, E. B. Maarouf, and E. Hannecart, *Synth. Met.*, **69**, 571 (1995).
56. E. B. Maarouf, D. Billaud, and E. Hannecart, *Mater. Res. Bull.*, **29**, 637 (1994).
57. P. S. Abthagir, K. Dhanalakshmi, and R. Saraswathi, *Synth. Met.*, **93**, 1 (1998).
58. R. Lazzaroni, A. D. Pryck, C. H. Debraisieux, J. Riga, J. Verbist, J. L. Brédas, J. Delhalle, and J. M. André, *Synth. Met.*, **21**, 189 (1987).
59. Z. Cai and G. Yang, *Synth. Met.*, **160**, 1902 (2010).
60. Z. Cai, X. Shi, and R. Zhan, *Mater. Lett.*, **92**, 271 (2013).
61. M. E. Argun, S. Dursun, M. Karatas, and M. Guru, *Bioresour. Technol.*, **99**, 8691 (2009).
62. J. C. Igwe, A. A. Abia, and C. A. Ibeh, *Int. J. Environ. Sci. Technol.*, **5**, 83 (2008).